

Absolute clock synchronization with a single time-correlated photon pair source over 10 km

JIANWEI LEE,¹ LIJIONG SHEN,¹ ADRIAN NUGRAHA UTAMA,¹ AND CHRISTIAN KURTSIEFER^{1,2,*}

¹Centre for Quantum Technologies, National University of Singapore, 3 Science Drive 2, Singapore 117543, Singapore

²Department of Physics, National University of Singapore, 2 Science Drive 3, Singapore 117551, Singapore

*christian.kurtsiefer@gmail.com

Abstract: We demonstrate a point-to-point clock synchronization protocol based on bidirectionally propagating photons generated in a single spontaneous parametric down-conversion (SPDC) source. Tight timing correlations between photon pairs are used to determine the single and round-trip times measured by two separate clocks, providing sufficient information for distance-independent absolute synchronization secure against symmetric delay attacks. We show that the coincidence signature useful for determining the round-trip time of a synchronization channel, established using a 10 km telecommunications fiber, can be derived from photons reflected off the end face of the fiber without additional optics. Our technique allows the synchronization of multiple clocks with a single reference clock co-located with the source, without requiring additional pair sources, in a client-server configuration suitable for synchronizing a network of clocks.

© 2022 Optica Publishing Group under the terms of the [Optica Publishing Group Publishing Agreement](#)

1. Introduction

Complementary to clock recovery schemes from data streams, absolute clock synchronization protocols, e.g. network time protocol (NTP), precision time protocol (PTP), two-way satellite time transfer (TWSTT), are widely-used to determine the offset between physically separated clocks [1–4]. By exchanging counter-propagating signals, and assuming a symmetric synchronization channel, parties estimate one-way propagation delays as half the round-trip time signals without characterizing their physical separation beforehand. Spatially separated parties then deduce their absolute clock offset by comparing signal propagation times measured with their devices with the expected propagation delay [5]. Recently, protocol implementations with entangled photon pairs suggest securing the synchronization channel by measuring non-local correlations – a technique inspired by entanglement-based quantum key distribution (QKD) [6–8]. With two independent Rubidium (Rb) clocks as references, the protocol has a demonstrated timing stability limited to the intrinsic instability of the clocks over 7 km [9], and is secure against symmetric-delay attacks [6]. However, to realize a bidirectional exchange of photons, these demonstrations required a photon pair source at each end of the synchronization channel, posing a resource challenge when synchronizing multiple clocks.

In this work, we experimentally demonstrate a bidirectional clock synchronization protocol where the synchronization channel is established with a 10 km optical fiber and a single entangled photon pair source. The round-trip time is sampled using time-correlation measurements between the detection times of photon pairs, with one photon of the pair back-reflected at the remote side using the end face of the fiber. We demonstrate a distance-independent synchronization of two separated clocks, referenced to independent Rubidium frequency standards. Already from a quite modest photon pair detection rate of 160 s^{-1} we obtain a precision sufficient to resolve clock offset fluctuations with an uncertainty of 88 ps in 100 s, consistent with the intrinsic frequency instability between our clocks.

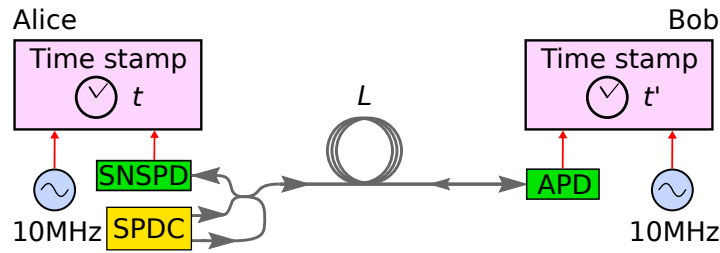


Fig. 1. Clock synchronization setup. Alice has a source of time-correlated photon pairs based on spontaneous parametric down-conversion (SPDC) and a single-photon nanowire photodetector (SNSPD). One photon of the pair is detected locally, while the other one is sent through a single mode fiber of length L to be detected on the remote side with Bob's InGaAs avalanche photodiode (APD). Times of arrival for all detected photons are recorded at each side with respect to the local clock, each locked to a rubidium frequency reference (10 MHz). Occasionally, a transmitted photon is reflected at the end face of the fiber back to Alice, allowing her to determine the round-trip time and derive the absolute offset between the clocks.

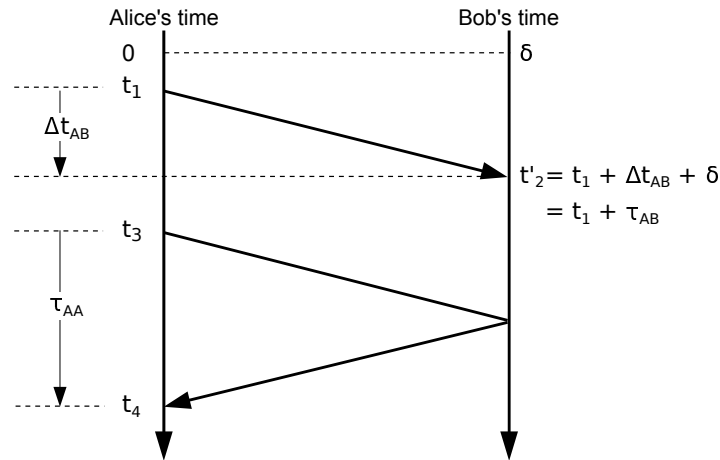


Fig. 2. Clock synchronization scheme. Alice and Bob measure detection times t and t' of photon pairs generated from Alice's source using local clocks. Detection times t_1 and t'_2 are associated with a time-correlated photon pair where one photon of the pair is transmitted to Bob, while t_3 and t_4 are associated with a pair where one of the photons is reflected at Bob back to Alice. The single-trip time τ_{AB} of photons in the synchronization channel, calculated from the time difference $t'_2 - t_1$, depends on the signal delay Δt_{AB} associated with the length of the channel, and the absolute clock offset δ between the clocks. The round-trip time τ_{AA} of the channel is estimated using $t_4 - t_3$. Assuming a symmetric delay channel, δ can be derived from τ_{AB} and τ_{AA} without *a priori* knowing Δt_{AB} .

46 2. Time synchronization protocol

47 The protocol involves two parties, Alice and Bob, connected by a single mode optical fiber (see
 48 Fig. 1). Alice has an SPDC source producing photon pairs, one photon is detected locally, while
 49 the other is sent and detected on the remote side. Occasionally, the transmitted photon undergoes
 50 Fresnel reflection ($R \approx 3.5\%$) at the end face of the fiber, and is eventually detected by Alice
 51 instead. Every photodetection event is time tagged according to a local clock which assigns time
 52 stamps t and t' at Alice and Bob, respectively.

53 Photon pairs emerging from SPDC are tightly time-correlated (≈ 100 fs) [10]. Thus, for an
 54 offset δ between the clocks, a propagation time Δt_{AB} from Alice to Bob, and Δt_{BA} in the other
 55 direction, the second-order correlation function [11] $G^{(2)}(\tau)$ of the time difference $\tau = t' - t$
 56 has a peak at

$$\tau_{AB} = \delta + \Delta t_{AB} \quad (1)$$

57 due to pairs detected at opposite ends of the channel, whereas for two photons detected by Alice
 58 at t and $t + \tau$, the auto-correlation function $R(\tau)$ will show a peak at

$$\tau_{AA} = \Delta t_{AB} + \Delta t_{BA}, \quad (2)$$

59 corresponding to the round-trip time of the channel. If the propagation times in the two directions
 60 are the same, $\Delta t_{AB} = \Delta t_{BA}$, the clock offset can be deduced directly from the positions of the
 61 two peaks using

$$\delta = \tau_{AB} - \frac{1}{2} \tau_{AA}, \quad (3)$$

62 independently of the propagation time Δt_{AB} . In this way, the protocol is inherently robust against
 63 symmetric changes in channel propagation times.

64 3. Experiment

65 A sketch of the experimental setup is shown in Fig. 1. Our photon pair source [12–14] is based
 66 on Type-0 SPDC in a periodically-poled crystal of potassium titanyl phosphate (PPKTP) pumped
 67 by a laser diode at 658 nm (Ondax, stabilized with holographic grating). The resulting photon
 68 pairs are degenerate at 1316 nm, close to the zero dispersion wavelength of the synchronization
 69 channel (SMF-28e, 10 km), with a bandwidth of ≈ 50 nm on either side of this wavelength [14].
 70 Signal and idler photons are efficiently separated using a wavelength division demultiplexer
 71 (WDM). Fiber beam splitters separate the photon pairs so that one photon is detected locally
 72 with a superconducting nanowire single-photon detector (SNSPD, optimized for 1550 nm), while
 73 the other photon is routed into the synchronization channel where it is detected on the remote
 74 side with an InGaAs avalanche photodiode (APD). The SNSPD has relatively low jitter (≈ 40 ps)
 75 compared to APDs (≈ 300 ps), and allows Alice to measure the round-trip time more accurately
 76 regardless of the choice of detector by the remote party. With a pump power of 2.5 mW focused
 77 to a beam waist of $140 \mu\text{m}$ at the centre of the crystal, we observed pair rates of 160 s^{-1} and
 78 8900 s^{-1} associated with the round-trip and single-trip propagation of photons, respectively.

79 Photon detection times t and t' at Alice and Bob are registered with a nominal resolution of
 80 ≈ 4 ps. We compute [15] the histograms $G^{(2)}(\tau)$ and $R(\tau)$ with a bin width of 62.5 ps, and
 81 observed coincidence peaks associated with the single-trip and round-trip propagating photons
 82 (FWHM = 905 ps and 950 ps, respectively). Figure 3 shows the respective histograms normalized
 83 to background coincidences when the two clocks are locked to a common rubidium frequency
 84 reference (Stanford Research Systems FS725), separated by a fiber spool of constant length
 85 $L = 10$ km. To deduce the clock offset, we first generate empirical models (Fig. 3, solid-lines) for
 86 the two coincidence peaks using 100 s of timestamp data – the models are used to fit subsequent
 87 histograms to extract peak positions τ_{AB} and τ_{AA} . With the peak positions, we then determine
 88 the clock offset using Eqs. 2 and 3.

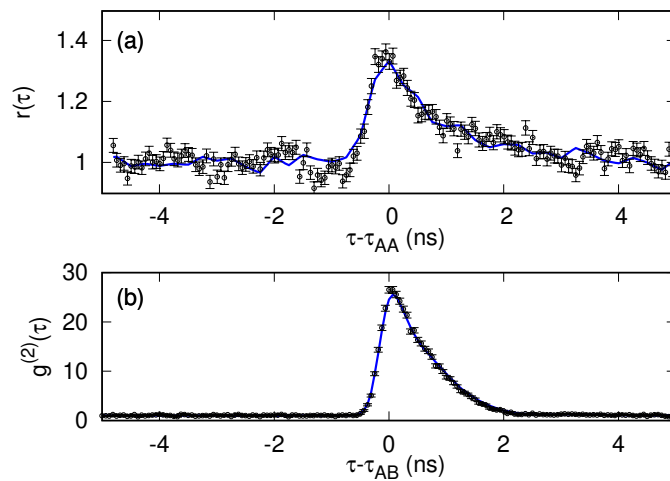


Fig. 3. Timing correlations showing coincidence peaks due to (a) round-trip and (b) single-trip propagation of photons in the synchronization channel. (a) $r(\tau)$: auto-correlation function $R(\tau)$ normalized to background coincidences extracted from Alice's timestamps acquired over 90 s. (b) $g^{(2)}(\tau)$: cross-correlation function $G^{(2)}(\tau)$ normalized to background coincidences extracted from Alice and Bob's timestamps acquired over 3 s. Solid lines: fits to heuristic model. τ_{AA} and τ_{AB} : peak positions of respective distributions. Error bars: propagated Poissonian counting statistics.

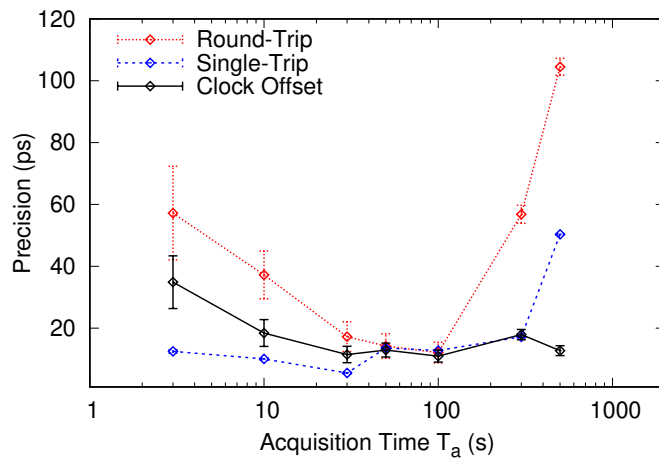


Fig. 4. Precision of the round-trip (red) and single-trip (blue) times, and the clock offset (black) between two clocks. Both clocks are locked to the same frequency reference. Error bars: precision uncertainty due to errors in determining the positions, τ_{AB} and τ_{AA} , of the coincidence peaks.

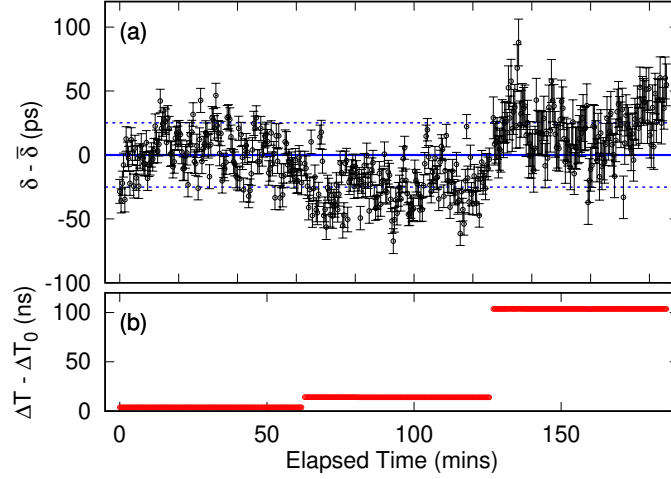


Fig. 5. (a) Measured offset δ between two clocks, both locked on the same frequency reference. The continuous line indicates the average offset $\bar{\delta}$. Error bars: precision uncertainty due to errors in determining the positions, τ_{AB} and τ_{AA} , of the coincidence peaks. Dashed lines: one standard deviation. (b) The round-trip time ΔT was changed using fiber lengths $L = L_0 = 10$ km, $L_0 + 1$ m, and $L_0 + 10$ m. $\Delta T_0 = 103.3 \mu\text{s}$.

89 To characterize the synchronization precision δt as a function of the acquisition time, we
90 measure the standard deviation of twenty offset measurements, each extracted from time stamps
91 recorded for a duration T_a . Figure 4 shows the precision of the measured offset, single-trip
92 (τ_{AB}) and round-trip times (τ_{AA}). We observe that the precision for the single and round-trip
93 times improves with T_a for timescales $\lesssim 100$ s, but deteriorates for longer timescales. We
94 attribute this effect to temperature-dependent ($\Delta T = 45$ mK over 1 min, 160 mK over 3 hours)
95 length fluctuations, given that the propagation delay variation [16] of our fiber is several
96 $10 \text{ ps km}^{-1} \text{ K}^{-1}$. However, we observe that these long-term fluctuations are suppressed in the
97 clock offset measurement with the distance-independent synchronization protocol.

98 For subsequent demonstrations, we set $T_a = 3$ s and 90 s for the single and round-trip time
99 measurements, obtaining a precision of 12 ps and 14 ps, respectively. Each 90 s window used
100 to evaluate the round-trip time thus contains thirty single-trip time measurements. For each
101 single-trip time value, we evaluate the clock offset using the round-trip time evaluated in the same
102 window. This results in a precision of 16 ps for the measured offset. Measuring the single-trip
103 delay with shorter T_a enables frequent measuring of $G^{(2)}(\tau)$, and is useful for tracking the
104 position of its coincidence peak (τ_{AB}) in the scenario where clocks are locked to independent
105 frequency references.

106 The minimum resolvable clock separation associated with the offset precision is 3.3 mm. To
107 demonstrate that the protocol is secure against symmetric channel delay attacks, we change the
108 propagation length over several meters during synchronization — three orders of magnitude
109 larger than the minimum resolvable length-scale.

110 4. Distance-independent clock synchronization with the same reference clock

111 To simulate a symmetric channel delay attack, we impose different propagation distances using
112 different fiber lengths. Figure 5 shows the measured offset δ and the round-trip time ΔT , with
113 an overall standard deviation of 26 ps, and an overall mean of $\bar{\delta}$. The sets of δ obtained for
114 $L = L_0 + 1$ m and $L_0 + 10$ m, with mean offsets $\bar{\delta} - 24(17)$ ps, and $\bar{\delta} + 20(20)$ ps, respectively,

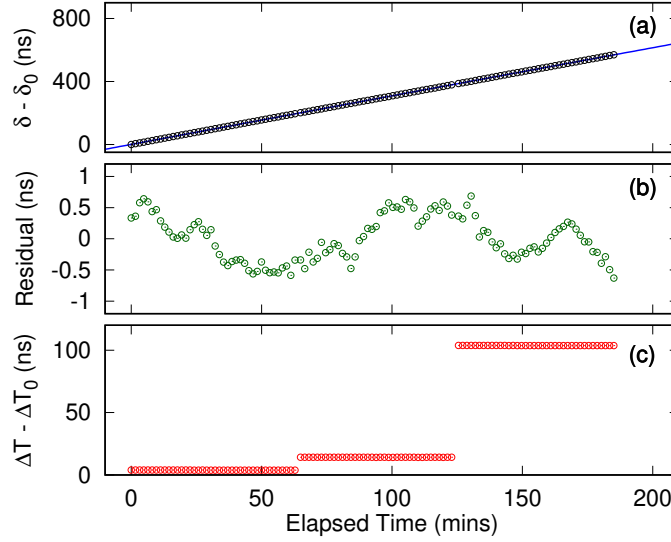


Fig. 6. (a) Measured offset δ between two clocks with different frequency references. Each value of δ was evaluated from measuring photon pair timing correlations for 3 s. The offset measured at the beginning is δ_0 . Continuous blue line: fit used to extract the relative frequency accuracy ($\approx 5.16 \times 10^{-11}$) between the clocks. (b) Residual of the fit fluctuates due to the intrinsic instability of the individual frequency references. (c) The round-trip time ΔT was changed using three different fiber lengths.

115 show significant overlap with those obtained with $L = L_0 = 10$ km with mean offset $\bar{\delta} + 1(17)$ ps.
 116 Comparing the additional mean offset of 19(26) ps to the additional single-trip delay (48.3 ns)
 117 expected for extending our optical channel from $L = L_0$ to $L_0 + 10$ m, our protocol suppresses the
 118 contribution of the additional propagation delay on the measured offset by a factor of $\approx 4 \times 10^{-4}$.

119 5. Distance-independent clock synchronization with independent clocks

120 To examine a more realistic scenario, we provide each time-stamping unit with an independent
 121 frequency reference (both Stanford Research Systems FS725), resulting in a clock offset that
 122 drifts with time $\delta \rightarrow \delta(t)$.

123 The frequency references each have a nominal frequency accuracy $d_0 < 5 \times 10^{-11}$, resulting in
 124 a relative accuracy $\sqrt{2} d_0$ between two clocks. We evaluate the offset from the time stamps every
 125 $T_a = 3$ s so that the maximum expected drift (< 212 ps) of the coincidence peak in $G^{(2)}(\tau)$ is
 126 smaller than its FWHM. This pseudo-stationary regime allows the peak positions to be extracted
 127 with the same fitting procedure used when the clocks are locked onto the same frequency
 128 reference [6].

129 We again simulate a symmetric channel delay attack using three different values of L . Figure 6
 130 shows the measured $\delta(t)$ which appears to follow a continuous trend over different round-trip
 131 times, indicating that the delay attacks were ineffective. Discontinuities in $\delta(t)$ correspond to
 132 periods when fibers were changed.

133 To verify that meaningful clock parameters can be extracted from $\delta(t)$ despite the attack, we
 134 fit the data to a parabola $at^2 + dt + b$, where a , d and b represent the relative aging, frequency
 135 accuracy and bias of the frequency references, respectively [17]. The resulting relative frequency
 136 accuracy between the clocks, $d = 5.1654(7) \times 10^{-11}$, agrees with the nominal relative frequency
 137 accuracy $\sqrt{2} d_0$ between our frequency references. The residual of the fit, $r(t)$ (Fig. 6(b)),

138 fluctuates [18] (Allan deviation = 2.2×10^{-12} , time deviation = 88 ps in 100 s) mainly due to the
139 intrinsic instabilities of our frequency references (2×10^{-12} in 100 s each).

140 6. Protocol Security

141 Although not demonstrated in this work, Alice and Bob can verify the origin of each photon by
142 synchronizing with polarization-entangled photon pairs and performing a Bell measurement to
143 check for correspondence between the local and transmitted photons. This proposal addresses
144 the issue of spoofing in current classical synchronization protocols [6, 8]. However, due to low
145 coincidence-to-accidental ratio associated with the round-trip time measurement (CAR=0.13),
146 this authentication scheme is only feasible for the single-trip time measurement (CAR=8.9).
147 Consequently, users can only authenticate photons traveling from Alice to Bob, and have to
148 assume that the synchronization channel has not been asymmetrically manipulated in order to
149 incorporate the round-trip time measurement in the clock offset calculation (Eqn. 3).

150 In addition, we also assumed that the photon propagation times in both directions were equal
151 ($\Delta t_{AB} = \Delta t_{BA}$). Without this assumption, the offset

$$\delta = \tau_{AB} - \tau_{AA} + \Delta t_{BA} \quad (4)$$

152 can no longer be obtained directly from the peak positions τ_{AB} and τ_{AA} .

153 We note that an adversary will be able to exploit both assumptions while evading detection by
154 passively rerouting photons traveling in opposite directions in the synchronization channel without
155 disturbing their polarization states [19]. This attack is based on the fact that the momentum and
156 polarization degree-of-freedom of our photons are separable, and remains a security loophole in
157 similar implementations [6, 7].

158 7. Conclusion

159 We have demonstrated a protocol for synchronizing two spatially separated clocks absolutely with
160 time-correlated photon pairs generated from SPDC. By assuming symmetry in the synchronization
161 channel, the protocol does not require *a priori* knowledge of the relative distance or propagation
162 times between two parties, providing security against symmetric channel delay attacks and
163 timing signal authentication via the measurement of a Bell inequality [8]. Compared to previous
164 implementations [6, 7], our protocol requires only a single photon pair source, relying on the
165 back-reflected photon to sample the round-trip time of the synchronization channel. This
166 arrangement allows multiple parties to synchronize with bidirectional signals with a single source.

167 With our protocol, we synchronize two independent rubidium clocks while changing their relative
168 separation, using telecommunication fibers of various lengths (≥ 10 km) as a synchronization
169 channel. Even with relatively modest detected coincidence rates (160 s^{-1}) used for the round-trip
170 time measurement, we obtained a precision sufficient to resolve clock offset fluctuations with a
171 time deviation of 88 ps in 100 s, consistent with the intrinsic frequency instabilities of our clocks.
172 The precision improves with detectors with lower timing jitter [7], brighter sources, or for a
173 transmission channel with insignificant dispersion (free space). Frequency entanglement may
174 also be leveraged to cancel dispersion non-locally, improving protocol precision over optical
175 channels in future work [7].

176 8. Backmatter

177 **Funding.** This research is supported by the National Research Foundation, Prime Minister's Office,
178 Singapore and the Ministry of Education, Singapore under the Research Centres of Excellence programme.

179 **Acknowledgments.** We thank S-Fifteen Instruments for assistance with the entangled photon pair source
180 and the InGaAs detector.

181 **Disclosures.** The authors declare no conflicts of interest.

182 **Data availability.** Data underlying the results presented in this paper are not publicly available at this time
183 due to their large file size (about 310 Gb) but may be obtained from the authors upon reasonable request.

184 References

- 185 1. W. Wenjun, D. Shaowu, L. Huanxin, and Z. Hong, “Two-way satellite time and frequency transfer: Overview, recent
186 developments and application,” in *2014 European Frequency and Time Forum (EFTF)*, (IEEE, 2014), pp. 121–125.
- 187 2. D. L. Mills, “Internet time synchronization: the network time protocol,” *IEEE Transactions on Commun.* **39**,
188 1482–1493 (1991).
- 189 3. “Ieee standard for a precision clock synchronization protocol for networked measurement and control systems,” *IEC*
190 61588:2009(E) pp. C1–274 (2009).
- 191 4. P. Moreira, J. Serrano, T. Wlostowski, P. Loschmidt, and G. Gaderer, “White rabbit: Sub-nanosecond timing
192 distribution over ethernet,” in *2009 International Symposium on Precision Clock Synchronization for Measurement,*
193 *Control and Communication*, (2009), pp. 1–5.
- 194 5. L. Narula and T. E. Humphreys, “Requirements for secure clock synchronization,” *IEEE J. Sel. Top. Signal Process.*
195 **12**, 749–762 (2018).
- 196 6. J. Lee, L. Shen, A. Cerè, J. Troupe, A. Lamas-Linares, and C. Kurtsiefer, “Symmetrical clock synchronization with
197 time-correlated photon pairs,” *Appl. Phys. Lett.* **114**, 101102 (2019).
- 198 7. F. Hou, R. Dong, R. Quan, X. Xiang, T. Liu, X. Yang, H. Li, L. You, Z. Wang, and S. Zhang, “Fiber-optic quantum
199 two-way time transfer with frequency entangled pulses,” *arXiv preprint arXiv:1812.10077* (2018).
- 200 8. A. Lamas-Linares and J. Troupe, “Secure quantum clock synchronization,” in *Advances in Photonics of Quantum*
201 *Computing, Memory, and Communication XI*, vol. 10547 (International Society for Optics and Photonics, 2018), p.
202 105470L.
- 203 9. R. Quan, H. Hong, W. Xue, H. Quan, W. Zhao, X. Xiang, Y. Liu, M. Cao, T. Liu, S. Zhang *et al.*, “Implementation
204 of field two-way quantum synchronization of distant clocks across a 7 km deployed fiber link,” *arXiv preprint*
205 *arXiv:2109.00784* (2021).
- 206 10. C.-K. Hong, Z.-Y. Ou, and L. Mandel, “Measurement of subpicosecond time intervals between two photons by
207 interference,” *Phys. review letters* **59**, 2044 (1987).
- 208 11. R. J. Glauber, “The quantum theory of optical coherence,” *Phys. Rev.* **130**, 2529 (1963).
- 209 12. Y. Shi, S. M. Thar, H. S. Poh, J. A. Grieve, C. Kurtsiefer, and A. Ling, “Stable polarization entanglement based
210 quantum key distribution over metropolitan fibre network,” *arXiv preprint arXiv:2007.01989* (2020).
- 211 13. A. Lohrmann, C. Perumangatt, A. Villar, and A. Ling, “Broadband pumped polarization entangled photon-pair
212 source in a linear beam displacement interferometer,” *Appl. Phys. Lett.* **116**, 021101 (2020).
- 213 14. J. A. Grieve, Y. Shi, H. S. Poh, C. Kurtsiefer, and A. Ling, “Characterizing nonlocal dispersion compensation in
214 deployed telecommunications fiber,” *Appl. Phys. Lett.* **114**, 131106 (2019).
- 215 15. C. Ho, A. Lamas-Linares, and C. Kurtsiefer, “Clock synchronization by remote detection of correlated photon pairs,”
216 *New J. Phys.* **11**, 045011 (2009).
- 217 16. M. Bousonville and J. Rausch, “Velocity of signal delay changes in fibre optic cables,” in *Proceedings of the Ninth*
218 *European Workshop on Beam Diagnostics and Instrumentation for Particle Accelerators (DIPAC)*, (2009).
- 219 17. G. Xu and Y. Xu, *GPS, Theory, Algorithms and Applications* (Springer Berlin Heidelberg, Berlin, Heidelberg, 2016).
- 220 18. W. J. Riley, *Handbook of frequency stability analysis* (US Department of Commerce, National Institute of Standards
221 and Technology, 2008).
- 222 19. J. Lee, L. Shen, A. Cerè, J. Troupe, A. Lamas-Linares, and C. Kurtsiefer, “Asymmetric delay attack on an
223 entanglement-based bidirectional clock synchronization protocol,” *Appl. Phys. Lett.* **115**, 141101 (2019).